ACCOUNTS
of chemical research

Synthesis, Structure, and Carbon Dioxide Capture Properties of Zeolitic Imidazolate Frameworks

ANH PHAN, CHRISTIAN J. DOONAN, FERNANDO J. URIBE-ROMO, CAROLYN B. KNOBLER, MICHAEL O'KEEFFE, AND OMAR M. YAGHI*

Center for Reticular Chemistry at California NanoSystems Institute, Department of Chemistry and Biochemistry, University of California—Los Angeles, 607 Charles E. Young Drive East, Los Angeles, California 90095

RECEIVED ON APRIL 6, 2009

CONSPECTUS

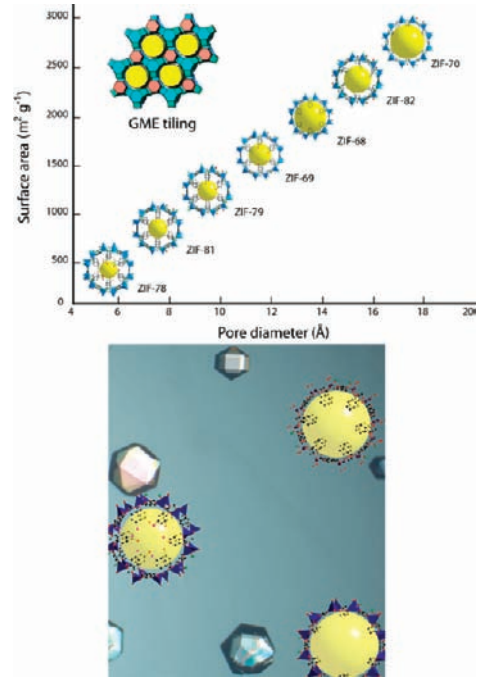

Zeolites are one of humanity's most important synthetic products. These aluminosilicate-based materials represent a large segment of the global economy. Indeed, the value of zeolites used in petroleum refining as catalysts and in detergents as water softeners is estimated at $350 billion per year. A major current goal in zeolite chemistry is to create a structure in which metal ions and functionalizable organic units make up an integral part of the framework. Such a structure, by virtue of the flexibility with which metal ions and organic moieties can be varied, is viewed as a key to further improving zeolite properties and accessing new applications.

Recently, it was recognized that the Si—O—Si preferred angle in zeolites (145°) is coincident with that of the bridging angle in the M—Im—M fragment (where M is Zn or Co and Im is imidazolate), and therefore it should be possible to make new zeolitic imidazolate frameworks (ZIFs) with topologies based on those of tetrahedral zeolites. This idea was successful and proved to be quite fruitful; within the last 5 years over 90 new ZIF structures have been reported. The recent application of high-throughput synthesis and characterization of ZIFs has expanded this structure space significantly: it is now possible to make ZIFs with topologies previously unknown in zeolites, in addition to mimicking known structures.

In this Account, we describe the general preparation of crystalline ZIFs, discussing the methods that have been developed to create and analyze the variety of materials afforded. We include a comprehensive list of all known ZIFs, including structure, topology, and pore metrics. We also examine how complexity might be introduced into new structures, highlighting how link—link interactions might be exploited to effect particular cage sizes, create polarity variations between pores, or adjust framework robustness, for example.

The chemical and thermal stability of ZIFs permit many applications, such as the capture of CO_2 and its selective separation from industrially relevant gas mixtures. Currently, ZIFs are the best porous materials for the selective capture of CO_2; furthermore, they show exceptionally high capacity for CO_2 among adsorbents operating by physisorption. The stability of ZIFs has also enabled organic transformations to be carried out on the crystals, yielding covalently functionalized isoreticular structures wherein the topology, crystallinity, and porosity of the ZIF structure are maintained throughout the reaction process. These reactions, being carried out on macroscopic crystals that behave as single molecules, have enabled the realization of the chemist's dream of using "crystals as molecules", opening the way for the application of the extensive library of organic reactions to the functionalization of useful extended porous structures.

Published on the Web 10/30/2009 www.pubs.acs.org/acr
10.1021/ar900116g

Introduction

Zeolitic imidazolate frameworks (ZIFs) are a new class of porous crystals with extended three-dimensional structures constructed from tetrahedral metal ions (e.g., Zn, Co) bridged by imidazolate (Im). The fact that the M−Im−M angle is similar to the Si−O−Si angle (145°) (Scheme 1) preferred in zeolites[1] has led to the synthesis of a large number of ZIFs with zeolite-type tetrahedral topologies. Given the small number of zeolites that have been made relative to the vast number of proposed tetrahedral structures, we anticipated that ZIF chemistry would allow access to a large variety of ZIFs by virtue of the flexibility with which the links and the metals can be varied. Indeed by combining metal salts with imidazole (ImH) in solution, a large number of crystalline ZIFs have been made; some of these possess topologies found in zeolites, and others have yet to be made as zeolites. Remarkably, ZIFs exhibit permanent porosity and high thermal and chemical stability, which make them attractive candidates for many applications such as separation and storage of gases.

In this Account, we present (1) the general synthesis of crystalline ZIFs and the great variety of tetrahedral nets that they adopt and the realization of this variety by development of high-throughput synthesis and characterization methods, (2) a comprehensive list of all known ZIFs including their structure, topology, and pore metrics, (3) the introduction of complexity by exploiting link−link interactions[2] to produce unusually large cages within ZIFs, incorporation of mixed links to give structures with a juxtaposition of polar and nonpolar pores, the exceptional robustness of their frameworks and the reproducible nature of their synthesis, which has led to a series of isoreticular (same topology) materials with controlled pore metrics, and the development of specific methods for carrying out organic reactions on the imidazolate links of the framework (isoreticular functionalization), and (4) the use of appropriate ZIF structures for the selective capture of CO_2.

Synthesis and General Structure

Generally, ZIFs are constructed by linking four-coordinated transition metals through imidazolate units to yield extended frameworks based on tetrahedral topologies. At the outset of our studies on ZIFs, only a small number of structures composed of divalent metal ions and imidazolate building units with topologies resembling those of zeolites had been reported; furthermore all of them, with the exception of three structures,[3−5] were nonporous or of a low symmetry, and their thermal and chemical stability had not been studied.[5−10]

SCHEME 1

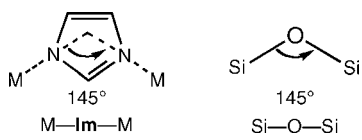

SCHEME 2

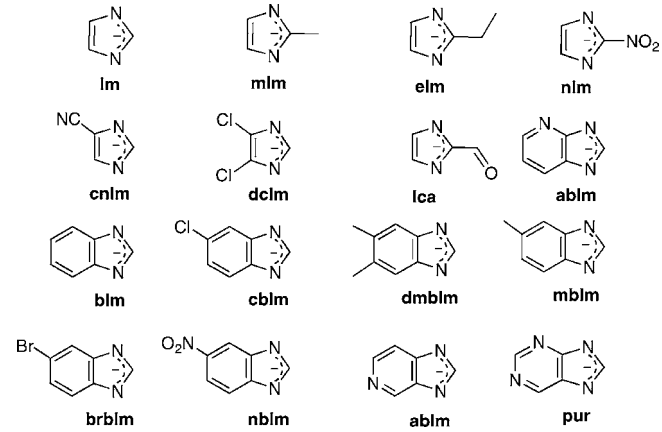

We developed a general synthetic procedure for obtaining porous crystalline ZIFs. It involves combining the desired hydrated transition metal salt and the ImH unit, of the kind shown in Scheme 2, in an amide solvent, such as DMF (*N*,*N*-dimethylformamide), and heating the solutions to temperatures ranging from 85 to 150 °C.[11] Under these conditions deprotonation of the linking ImH is achieved by amines resulting from the thermal degradation of the solvent. Typically, upon cooling, crystals are obtained in moderate to high yields (50−90%). The molar ratio and concentration of the metal ion and link and the temperature of the reaction are critically important for achieving monocrystalline materials suitable for single-crystal X-ray diffraction studies. In addition to providing the requisite bridging angle of 145° (Scheme 1) for synthesizing zeolite-type structures, the bridging Im unit is suspected to play a secondary role by directing the topology through link−link interactions.[12,13] This was exploited by employing functionalized Im links (Scheme 2) in the synthesis using microreactions and high-throughput synthesis and characterization involving the following synthetic protocol: (1) automated mixing of the reactants in varying concentration into microplate wells, (2) heating of these mixtures to produce crystalline ZIFs, (3) automated optical imaging of the individual wells, and (4) automated screening for crystalline specimens by collection of X-ray powder diffraction patterns for each of the wells. This was followed by single-crystal X-ray diffraction studies on the samples exhibiting new phases. Generally, most of the wells contain single-phase materials, and notably we find that often the microreaction conditions are scalable to gram quantities. In cases where such scale up was not possible, systematic variation of reactant concentration

and temperature and on occasion running the reactions in closed vessels has resulted in a scalable synthesis.[14,15] With these methods, it was possible to target specific topologies, discover previously unknown topologies, and optimize crystallization conditions for the synthesis of isoreticular materials based on a given topology.

ZIF Structures and the Zeolite Problem

Table 1 shows a comprehensive list of the topologies and summarizes the structural properties of all reported ZIFs. A variety of ZIFs have been synthesized that possess the zeolite topologies **ANA**, **BCT**, **DFT**, **GIS**, **GME**, **LTA**, **MER**, **RHO** and **SOD** (Figure 1). Among these, 15 structures (ZIF-60−62, -68−70, -73−76, and -78−82) form single-phase materials that are synthesized from mixed linkers.[14,16]

Notably these heterolink materials add functional complexity garnered by introducing another organic moiety into the backbone of the framework. ZIF structures also consist of nets that are not purely tetrahedral. For example (ZIF-5), $In_2Zn_3(Im)_{12}$ is comprised of In(III) and Zn(II) in octahedral and tetrahedral coordination environments, respectively, and the framework has the same topology as the (4,6)-coordinated **gar** net defined by the 4- and 6-coordinated atoms in the garnet structure such as Al and Si in $Ca_3Al_2Si_3O_{12}$.[11] In the ZIF with the CCDC code BETHUE with stoichiometry $Cu_2(Im)_3$, one copper atom is 4-coordinated and the other [clearly Cu(I)] is 2-coordinated to give a structure with a (2,4)-coordinated net. Recently, ZIFs have been reported in which two Zn are replaced with Li and B or with 4-coordinated tetrahedral Cu(I) and B.[12] ZIF-95 and ZIF-100 display unprecedented structural complexity and novel topologies termed **poz** and **moz**, respectively; in the latter, one vertex (out of ten different kinds) is 3-coordinated. These ZIFs have immense and complex cages; in particular, the most notable aspect of the ZIF-100 structure is a giant cage with 264 vertices assembled from 7524 atoms: 264 Zn, 3604 C, 2085 H, 26 O, 1030 N, and 515 Cl. The outer and inner sphere diameters measure 67.2 and 35.6 Å, respectively (a sphere fit from the centroid of the cage to the van der Waals surface of the cage's wall is used to determine the inner sphere diameter); in comparison the corresponding distances in the faujasite supercage in zeolite **FAU** are 18.1 and 14.1 Å, and the diameter of C_{60} is 10.5 Å (Figure 2).[15]

We call attention to some generalizations about the observed ZIF framework topologies and a comparison with zeolites. Noted first is that all zeolite nets found in ZIFs are vertex-transitive (uninodal). Table 1 includes 105 ZIFs that have structures based on 3-periodic 4-coordinated nets; 84 (84%) of these have uninodal nets. Or again of the same subset, there are 27 structure types of which 18 (68%) are uninodal; of these 18 only 4 (**frl**, **lcs**, **neb** and **zni**) have not been observed before in zeolites or in other aluminosilicates or related materials. The remaining nine framework types have respectively two, two, three, four, four, four, five, six, and six kinds of vertices and are previously unobserved topologies. The distribution of zeolite framework types is rather different. The *Atlas of Zeolite Framework Types* lists 180 4-coordinated topologies of which only 21 (26%) are uninodal, and there are a number with 12 or more topologically distinct kinds of vertices including one (**TUN**) with 24 kinds of vertices.[17]

Now, given the fact that the number of possible structure types increases exponentially with the number of vertices, one expects the number of possible zeolites with, say, up to 12 kinds of vertices to be at least millions, or more likely, vastly greater. The "zeolite problem" is this: zeolite synthesis has been an active area of research for 50 years with expenditure of thousands of person-years, yet only a tiny fraction of those potential zeolites have been found. One must conclude either that most of the purported potential zeolite structures are not suitable for some unknown reason or, surely more likely, that a good *general* method of synthesizing zeolites has yet to be discovered. We feel that the fact that so many ZIFs have been discovered in such a short time may lead to clues, the interactions between the organic building blocks in combination with reaction parameters such as temperature and solvent mixture, to a more general method of zeolite (*sensu stricto*) discovery. In any event, there is clearly an enormously rich field of synthetic materials chemistry waiting to be exploited. It is interesting that just as the most dense zero pressure phase, quartz, is the most stable for silicates, the most dense topology (**zni**) is calculated to be the most stable of unsubstituted imidazolates.[18]

Structural Complexity in ZIFs

We have observed that ZIF net topologies are directed through Im link−link interactions in combination with the solvent composition.[13,14] This important design feature demonstrated the potential for a systematic approach to further developing this new class of porous crystals. As a consequence, new topologies have been achieved through the judicious choice of sterically bulky links that prevent the formation of known topologies. For example, analysis of structural models of ZIFs formed from 2-methylimidazolate (mIm) and benzimidazolate (bIm), which form **SOD** and **RHO** type topologies, respectively,[11] indicated that substitution of the 4- and 5-positions of the

TABLE 1. Composition, CCDC Code, Structure, and Topology Parameters of All Reported ZIFs[a]

name	composition[b]	CCDC code[c]	RCSR topology[e]	zeolite code	T/V^f(T/nm^3)	$d_a{}^g$ (Å)	$d_p{}^h$ (Å)	ref
ZIF-14	$Zn(eIm)_2$	MECWIB	**ana**	**ANA**	2.57	2.2	2.2	4, 14
—[d]	$Co(Im)_2$	EQOCES01	**cag**	—[d]	3.40	2.4	2.4	31
ZIF-62	$Zn(nIm)_2$	GIZJOP	**cag**	—[d]	3.58	1.4	1.3	14
—[d]	$Co(Im)_2$	NAFGOR	**cag**	—[d]	3.64	1.0	1.0	31
ZIF-4	$Zn(Im)_2$	VEJYUF	**cag**	—[d]	3.68	2.0	2.1	11
—[d]	$Zn(Im)_2$	VEJYUF01	**cag**	—[d]	3.66	0.8	0.8	26
TIF-4	$Zn(Im)_{1.5}(mbIm)_{0.5}$	701064	**cag**	—[d]	3.46	2.0	6.9	38
—[d]	$Zn(Im)_2$	EQOCOC	**coi**	—[d]	4.73	2.5	6.0	8
—[d]	$Co(Im)_2$	IMZYCO	**coi**	—[d]	4.71	2.5	6.0	28
ZIF-64	$Zn(Im)_2$	GITTEJ	**crb**	**BCT**	3.62	2.5	7.9	14
—[d]	$Fe(mIm)_2$	LODCUC	**crb**	**BCT**	4.18	4.8	8.0	6
—[d]	$Co(Im)_2$	NAFGOR01	**crb**	**BCT**	3.62	0.9	3.0	31
ZIF-1	$Zn(Im)_2$	VEJYEP	**crb**	**BCT**	3.64	6.3	6.94	11
—[d]	$Zn(Im)_2$	VEJYEP01	**crb**	**BCT**	3.63	2.2	2.2	26
ZIF-2	$Zn_2(Im)_4$	VEJYIT	**crb**	**BCT**	2.80	6.4	6.9	11
—[d]	$Zn(Im)_2$	VEJYIT01	**crb**	**BCT**	2.78	5.4	5.7	26
—[d]	$Pr(Im)_5$	LEMVOP	**crs**	—[d]	2.19	1.6	1.6	37
—[d]	$Zn(Im)_2$	HIFVOI	**dft**	—[d]	2.58	6.6	9.6	26
ZIF-3	$Zn_2(Im)_4$	VEJYOZ	**dft**	—[d]	2.66	4.6	6	11
ZIF-23	$Zn(4abIm)_2$	MIHHOB	**dia**	—[d]	3.32	1.1	4.2	13
—[d]	$Cd_2(HIm)_3(Im)$	VIGHID	**dia**	—[d]	2.90	0.7	1.7	38
—[d]	$Fe(4abIm)_2$	XASGON	**dia**	—[d]	3.21	0.2	1.8	34
—[d]	$Fe(biIm)_2$	ZIMMEN	**dia**	—[d]	3.02	0.2	2.8	39
—[d]	$Hg(Im)_2$	BAYPUN	**dia-c**	—[d]	5.17	1.0	5.3	29
—[d]	$Cd(Im)_2$	BAYQAU	**dia-c**	—[d]	5.14	0.8	6.0	29
—[d]	$Cd(Im)_2$	BAYQAU01	**dia-c**	—[d]	5.13	2.0	3.3	8
—[d]	$Cd(Im)_2$	BAYQAU02	**dia-c**	—[d]	5.13	2.0	3.3	30
BIF-2Li	$LiB(mIm)_4$	699084	**dia-c-b**	—[d]	4.23	2.4	2.4	12
BIF-2Cu	$CuB(mIm)_4$	703703	**dia-c-b**	—[d]	4.16	2.6	2.6	12
BIF-6	$CuBH(im)_3$	697962	**fes**	—[d]	7.05	1.3	2.2	12
ZIF-73	$Zn(nIm)_{1.74}(mbIm)_{0.26}$	GITVOV	**frl**	—[d]	3.20	1.0	1.0	14
ZIF-77	$Zn(nIm)_2$	GITWIQ	**frl**	—[d]	3.23	2.9	3.6	14
ZIF-5	$Zn_3In_2(Im)_{12}$	VEJZAM	**gar**	—[d]	1.51	1.7	3.03	11
ZIF-6	$Zn(Im)_2$	EQOCOC01	**gis**	**GIS**	2.31	1.5	3.03	11
ZIF-74	Zn(mbIm)(nIm)	GITVUB	**gis**	**GIS**	2.67	1.2	2.6	14
ZIF-75	Co(mbIm)(nIm)	GITWAI	**gis**	**GIS**	2.67	1.2	2.62	14
—[d]	$Zn(Im)_2$	HIFVUO	**gis**	**GIS**	2.47	5.2	8.6	26
TIF-5Zn	Zn(Im)(dmbIm)	701066	**gis**	**GIS**	2.70	1.0	6.0	36
TIF-5Co	Co(Im)(dmbIm)	701065	**gis**	**GIS**	2.70	0.7	5.0	36
ZIF-68	Zn(bIm)(nIm)	GITTUZ	**gme**	**GME**	2.11	7.5	10.3	14
ZIF-69	Zn(cbIm)(nIm)	GITVAH	**gme**	**GME**	2.10	4.4	7.8	14
ZIF-70	$Zn(Im)_{1.13}(nIm)_{0.87}$	GITVEL	**gme**	**GME**	2.11	13.1	15.9	14
ZIF-78	Zn(nbIm)(nIm)	—[d]	**gme**	**GME**	2.08	3.8	7.1	16
ZIF-79	Zn(mbIm)(nIm)	—[d]	**gme**	**GME**	2.10	4.0	7.5	16
ZIF-80	Zn(dcIm)(nIm)	—[d]	**gme**	**GME**	2.07	9.8	13.2	16
ZIF-81	Zn(brbIm)(nIm)	—[d]	**gme**	**GME**	2.08	3.9	7.4	16
ZIF-82	Zn(cnIm)(nIm)	—[d]	**gme**	**GME**	2.09	8.1	12.3	16
ZIF-72	$Zn(dcIm)_2$	GIZJUV	**lcs**	—[d]	3.16	1.9	1.9	14
ZIF-76	Zn(Im)(cbIm)	GITWEM	**lta**	**LTA**	1.03	1.9	1.9	14
ZIF-20	$Zn(pur)_2$	MIHHAN	**lta**	**LTA**	2.04	2.8	15.4	13
ZIF-21	$Co(pur)_2$	MIHHER	**lta**	**LTA**	2.04	2.8	15.4	13
ZIF-22	$Zn(5abIm)_2$	MIHHIV	**lta**	**LTA**	2.02	2.9	14.8	13
—[d]	$Cd(Im)_2(bipy)$	DAYVIJ	**mab**	—[d]	2.67	1.1	3.2	40
usf-ZMOF	$In_5(Imdc)_{10}$	690432	**med**	—[d]	1.94	4.3	9.7	35
ZIF-60	$Zn_2(Im)_3(mIm)$	GITSUY	**mer**	**MER**	2.24	7.2	9.4	14
ZIF-10	$Zn(Im)_2$	VEJZIU	**mer**	**MER**	2.25	8.2	12.2	14
—[d]	$Cu(Im)_2$	CUIMDZ03	**mog**	—[d]	4.97	1.3	3.5	9
—[d]	$Fe_3(Im)_6$	IMIDFE	**mog**	—[d]	4.18	1.9	3.1	41
—[d]	$Fe_3(Im)_6$	IMIDFE01	**mog**	—[d]	4.12	1.9	3.1	33
—[d]	$Mn_3(Im)_6$	IMIDZA	**mog**	—[d]	3.97	2.0	3.3	27
ZIF-100	$Zn_{20}(cbIm)_{39}(OH)$	668215	**moz**	—[d]	1.29	3.4	35.6	15
—[d]	$Co(Im)_2$	EQOBUH	**neb**	—[d]	3.82	0.6	6.7	8
—[d]	$Co(Im)_2$	EQOCES	**neb**	—[d]	3.61	1.8	7.1	8
—[d]	$Co(Im)_2$	EQOCIW	**neb**	—[d]	3.67	1.6	6.9	8
—[d]	$Co_5(Im)_{10}$	AFIXAO	**nog**	—[d]	3.50	4.1	5.5	7
—[d]	$Co_2(Im)_4$	AFIXAO01s	**nog**	—[d]	3.50	3.9	5.5	8
—[d]	$Co_5(Im)_{10}$	AFIXES	**nog**	—[d]	3.51	3.5	5.9	7
—[d]	$Zn(Im)_2$	HIFWAV	**nog**	—[d]	3.45	4.7	8.2	26
TIF-3	Zn(Im)(mbIm)	701063	**pcb**	**ACO**	2.77	2.2	6.2	36

TABLE 1. Continued

name	composition[b]	CCDC code[c]	RCSR topology[e]	zeolite code	T/V[f] (T/nm^3)	d_a[g] (Å)	d_p[h] (Å)	ref
ZIF-95	$Zn(cbIm)_2$	668214	**poz**	—[d]	1.51	3.7	24	15
—[d]	$Fe(mIm)_2$	CAGLIF	**qtz**	—[d]	3.61	2.6	6.0	42
ZIF-71	$Zn(dcIm)_2$	GITVIP	**rho**	**RHO**	2.06	4.2	16.5	14
—[d]	$Zn_2(eIm)_4$	MECWOH	**rho**	**RHO**	1.92	1.3	21.6	4, 5
rho-ZMOF	$In(Imdc)_2$	TEFWIL	**rho**	**RHO**	1.60	5.7	26.9	3
ZIF-11	$Zn(bIm)_2$	VEJZOA	**rho**	**RHO**	2.02	3	14.6	11
ZIF-12	$Co(bIm)_2$	VEJZUG	**rho**	**RHO**	2.02	3	14.6	11
ZIF-90	$Zn(Ica)_2$	693596	**sod**	**SOD**	2.33	3.5	11.2	21
—[d]	$Zn(bIm)_2$	AKUGES	**sod**	**SOD**	2.62	2.4	5.2	5, 10
—[d]	$Cu(Im)_2$	CUIMDZ01	**sod**	**SOD**	4.52	4.6	7.3	9
ZIF-65	$Co(nIm)_2$	GITTIN	**sod**	**SOD**	2.33	3.4	10.4	14
ZIF-67	$Co(mIm)_2$	GITTOT	**sod**	**SOD**	2.46	3.4	11.6	14
—[d]	$Zn(mIm)_2$	MECWEX	**sod**	**SOD**	2.44	3.0	14.2	4
—[d]	$Zn(Im\text{-}d5)_2$	OFERUN	**sod**	**SOD**	2.45	3.1	14.2	25
sod-ZMOF	$In(Imdc)_2$	TEFWOR	**sod**	**SOD**	2.05	1.2	8.1	3
ZIF-9	$Co(bIm)_2$	VEJZEQ	**sod**	**SOD**	2.51	2.9	4.31	10
ZIF-7	$Zn(bIm)_2$	VELVIS	**sod**	**SOD**	2.49	2.9	4.31	10
ZIF-8	$Zn(mIm)_2$	VELVOY	**sod**	**SOD**	2.45	3.4	11.6	10
ZIF-91	$Zn(hmIm)_2$	—[d]	**sod**	**SOD**	2.33	3.2	11	21
ZIF-92	$Zn(heIm)_2$	—[d]	**sod**	**SOD**	2.33	0	5.2	21
BIF-3Li	$LiB(mIm)_2$	703704	**sod-b**	**SOD**	2.91	2.7	10	12
BIF-3Cu	$CuB(mIm)_2$	697959	**sod-b**	**SOD**	2.92	2.7	9.9	12
BIF-8	$CuBH(eim)_3$	697964	**srs-c-b**	—[d]	4.62	0.8	4.2	12
BIF-7	$CuBH(mIm)_3$	697963	**ths-c-b**	—[d]	5.26	1.7	5.5	12
TIF-1Zn	$Zn(dmbIm)_2$	682400	**zea**	—[d]	1.61	3.0	4.1	43
TIF-1Co	$Co(dmbIm)_2$	—[d]	**zea**	—[d]	1.61	3.0	4.1	43
TIF-2	$Zn(Im)_{1.10}(mbIm)_{0.9}$	701062	**zeb**	—[d]	2.21	9.6	10.0	36
—[d]	$Zn(Im)_2$	HICGEG	**zec**	—[d]	2.96	5.0	5.0	26
ZIF-61	$Zn(Im)(mIm)$	GITTAF	**zni**	—[d]	4.62	0.7	0.7	14
—[d]	$Zn(Im)_2$	IMIDZB	**zni**	—[d]	4.66	3.6	3.6	27
—[d]	$Co(Im)_2$	IMZYCO01	**zni**	—[d]	4.67	3.7	3.7	8
BIF-1Li	$LiB(Im)_2$	693499	**zni-b**	—[d]	5.48	3.0	4.4	12
BIF-1Cu	$CuB(Im)_2$	693500	**zni-b**	—[d]	5.56	2.9	3.7	12
—[d]	$CuCu(Im)_3$	BETHUE	—[d]	—[d]	7.02	2.1	2.8	5, 32
BIF-4	$CuCu[B(bIm)_4]_2$	697960	—[d]	—[d]	3.01	0.7	3.6	12
BIF-5	$Cu_3I[B(bIm)_4]_2$	697961	—[d]	—[d]	2.53	2.6	3.3	12

[a] For method of analysis, see ref 44. [b] Formula excluding guests. [c] Deposition number was used where the CCDC code is unavailable. [d] The name, RCSR symbols, and zeolite symbols are not applicable or that the structure, CCDC code, and deposition number are not yet available. [e] For a description of RCSR symbols, see ref 45. [f] T/V is the density of metal atoms per unit volume. [g] d_a is the diameter of the largest sphere that will pass through the pore. [h] d_p is the diameter of the largest sphere that will fit into the cages without contacting the framework atoms. Pore metrics measurements exclude guests.

benzene unit of bIm provides sufficient steric encumbrance to prevent the formation of a structure with the **RHO** topology.[13] Indeed, by employing 5-chlorobenzimidazole as the organic building block, two new ZIFs, ZIF-95 and ZIF-100, were obtained. The salient features of these materials are their unusual structural complexity and giant cages (*vide supra*). In addition to their unique structures, these ZIFs also show exceptional CO_2 adsorption properties (Table 2).[15]

High-throughput methods were used to introduce an additional degree of complexity into ZIFs by employing mixtures of Im links (heterolinks).[14] Two different types of Im linker, especially those with a side chain, for example, $-NO_2$ (nIm) or $-CH_3$ (mIm), or an aromatic ring linker have been employed in the successful synthesis of ZIFs with **MER**, **GIS**, **GME**, and **LTA** topologies. These ZIFs have a 3D pore system in which hydrophilic and hydrophobic channels are found alternating in the crystal. A number of tetrahedral topologies such as **cag** and **frl**, which are yet to be found in zeolites, have been found by using heterolinks.[14] Heterolinks of brbIm, bIm, cnIm, cbIm, dcIm, Im, mbIm, nIm, and nbIm were used to make a series of isoreticular materials (ZIF-68−70 and ZIF-78−82); all having the GME topology.[14,16] It is worth noting that the **GME** topology is the only one found in ZIFs that has both large pores and large windows (Figure 1).

Many ZIFs have unusual chemical stability for metal−organic frameworks.[11,14−16] For example, ZIF-8 can be boiled in water, alkaline solutions, and refluxing organic solvents without loss of crystallinity and porosity.[11] Additionally, as anticipated for structures formed from robust links, their frameworks display high thermal stability (up to 500 °C).[11,14−16] The chemical stability of ZIFs in both aqueous and organic media provides a foundation for carrying out covalent modifications on the Im links of the frameworks without changing the underlying topology of the ZIF structures (isoreticular covalent functionalization) as has recently been demonstrated in MOF chemistry.[19,20] Accordingly, covalent

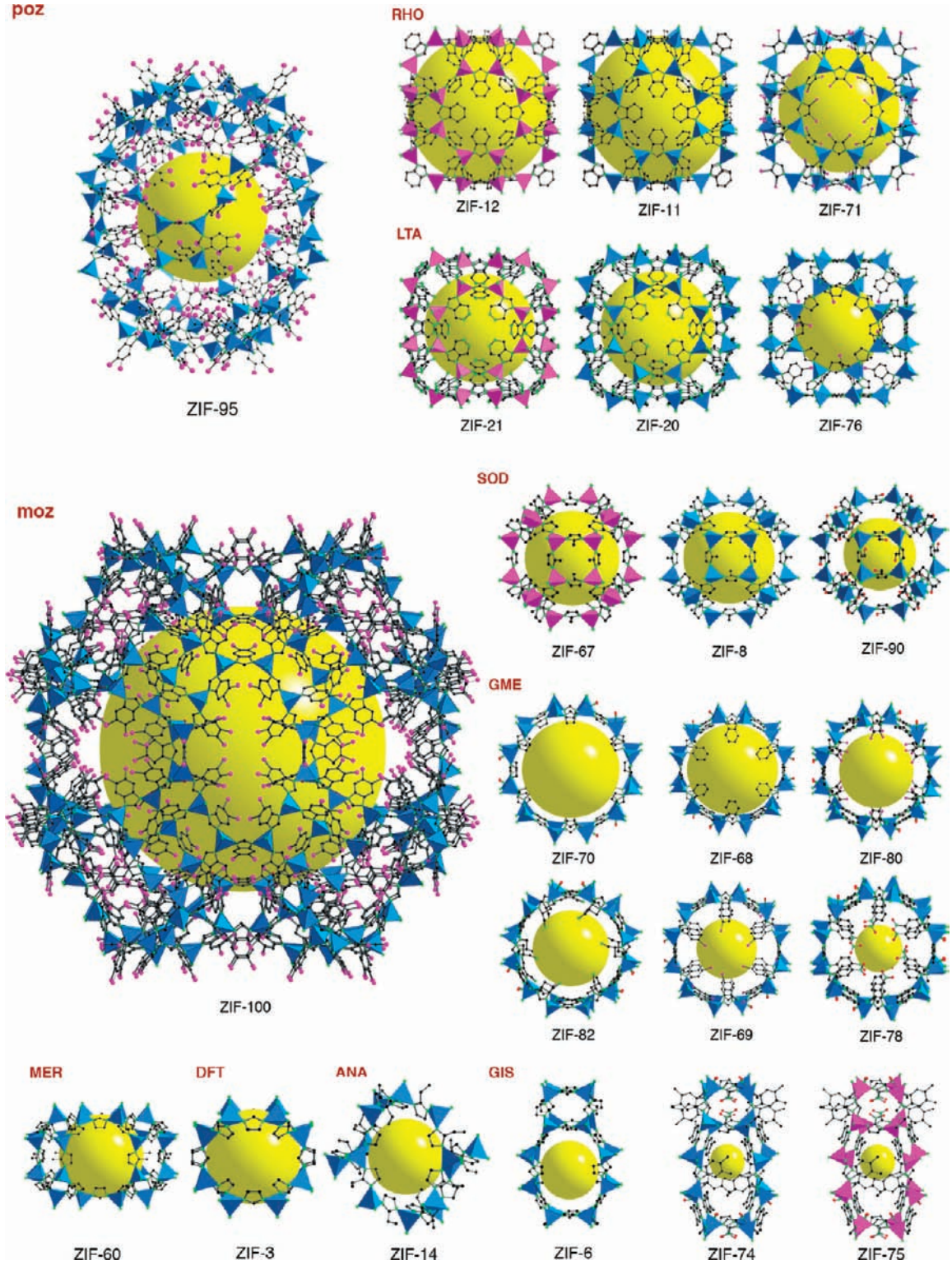

FIGURE 1. Crystal structures of ZIFs presented in this paper and grouped according to their topology (three-letter symbol).[17,45] The largest cage in each ZIF is shown with ZnN_4 in blue and CoN_4 in pink polyhedra, and the links in ball-and-stick presentation. The yellow ball indicates space in the cage. H atoms are omitted for clarity (C, black; N, green; O, red; Cl, pink). Supporting Information is available to view larger high-resolution images of crystal structures of ZIFs.

transformations of the organic links of ZIF-90, which possess aldehyde functionality in the 2-position of the imidazole unit, were recently effected. Two common organic reactions were carried out; reduction of the aldehyde to an alcohol with $NaBH_4$ and the formation of an imine bond by reaction with ethanolamine in 80% and quantitative yields, respectively

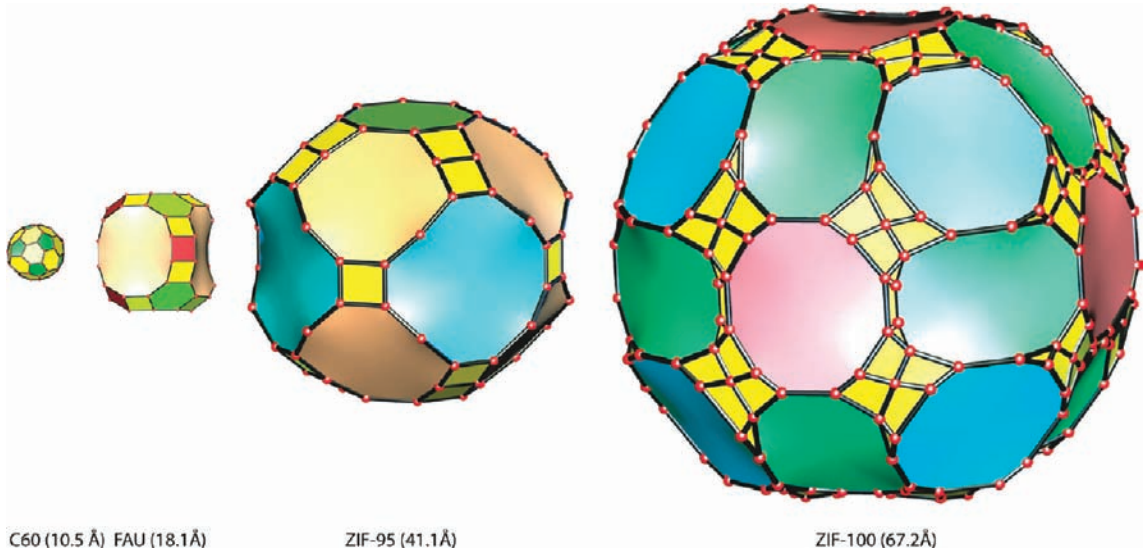

FIGURE 2. The cages in ZIF-95 and -100 are shown as natural tiling. The outer sphere diameters of ZIF-95 and -100 are in comparison with the corresponding distances in the faujasite (FAU) supercage in zeolite and in C_{60}. Zn atoms are represented by red spheres in ZIF-95 and ZIF-100.

TABLE 2. ZIF Surface Area, CO_2 Uptake, and Separation Selectivity for ZIF-68−70, -78, -79, -81, -95, and -100

material	BET ($m^2\ g^{-1}$)	CO_2 ($cm^3\ g^{-1}$)	CO_2 ($cm^3\ cm^{-3}$)	CO_2/CO	CO_2/CH_4	CO_2/N_2	CO_2/O_2
ZIF-95	1050	19.7	19.2	11.4 ± 1.1	4.3 ± 0.4	18 ± 1.7	—[b]
ZIF-100	595	32.6[a]	28.2[a]	17.3 ± 1.5	5.9 ± 0.4	25 ± 2.4	—[b]
ZIF-78	620	51.5	60.2	—[b]	10.6	50.1	47.7
ZIF-81	760	38.2	49.3	—[b]	5.7	23.8	27.9
ZIF-79	810	33.5	36.1	—[b]	5.4	23.2	22.2
ZIF-69	950	40.6	49.2	20.9	5.1	19.9	18.0
ZIF-68	1090	37.6	39.9	19.2	5.0	18.7	19.1
ZIF-82	1300	52.7	49.3	—[b]	9.6	35.3	34.1
ZIF-70	1730	55.0	45.4	37.8	5.2	17.3	16.7
BPL carbon[c]	1150	46.8	22.5	7.5	3.9	17.8	18.6

[a] Measured at 273 K. [b] No available data for the gas pair. [c] BPL carbon is used for comparison.

(Figure 3). A noteworthy aspect of this work is that subsequent to both transformations the crystallinity of the ZIF material was maintained.[21] This remarkable transformation makes the concept of using crystals as molecules a reality in ZIF chemistry and opens the way for performing organic chemistry on ZIFs.

Applications to Separations and Carbon Dioxide Selective Capture

ZIFs exhibit exceptional uptake capacities for CO_2 and can selectively separate CO_2 from industrially relevant gas mixtures. A series of ZIFs (ZIF-68, -69, -70, -78, -79, -81, -82, -95, and -100) have been examined for their potential to separate CO_2 from CH_4, CO, O_2, and N_2 (Table 2).[14−16] These mixtures are associated with processes involving natural-gas purification/combustion, landfill gas separation, and steam-methane reforming.[22] The CO_2 adsorption isotherms of ZIF-68, -69, and -70 show steep uptakes in the low-pressure regions indicating a high gas affinity; furthermore all aforementioned ZIFs also possess a high CO_2 uptake capacity. For example, we calculated that 1 L of ZIF-69 can store 82.6 L of CO_2 at 273 K. Indeed ZIF-69, the best-performing ZIF, displays a superior ability to store CO_2 in comparison to the industrially utilized adsorbent BPL carbon.[14] In addition to the significant gas uptake, the isotherms all display complete reversibility, a necessary property for a selective CO_2 adsorbent. Metal−organic frameworks (MOFs) are a class of crystalline, porous materials that have also demonstrated high uptake capacities for CO_2 and thus make for an interesting comparison to ZIFs.[23] Given that both ZIFs and MOFs can hold significantly large amounts of CO_2, other aspects of their physical properties need to be considered. For example, the relatively high chemical stability of ZIFs compared with MOFs makes them excellent candidates for industrial use. Furthermore, ZIFs have been shown to have a high affinity for CO_2 at low pressures (at 298 K and 1 atm, MOF-177 has a maximum uptake of 7.60 L/L CO_2 while ZIF-69 has a capacity of 82.6 L/L), which is relevant for a pressure swing adsorption

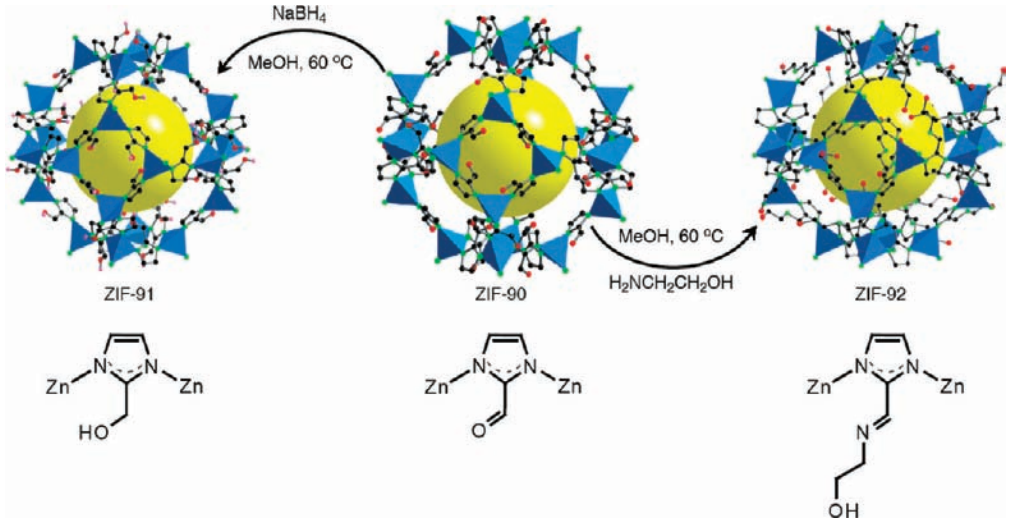

FIGURE 3. Isoreticular functionalization of ZIFs: crystal structure of ZIF-90 transformed to ZIF-91 by reduction with $NaBH_4$ and to ZIF-92 by reaction with ethanolamine. The yellow ball indicates space in the cage. H atoms are omitted for clarity, except the H of an alcohol group in ZIF-91 (C, black; N, green; O, red; Cl, pink).

type process for CO_2 capture.[24] In addition, ZIFs show greater selectivity than MOFs for CO_2 from other relevant flue gases (such as CO).[14] Due to these intrinsic differences in their physical and gas adsorption properties, we believe that ZIFs are preferable to MOFs for industrial application, especially given the importance of gas selectivity in CO_2 capture, because CO_2 does not come in pure form but rather as in flue gas (mixture of gases).[22]

Breakthrough experiments further support the affinity of the reported ZIFs for CO_2 by showing complete retention of CO_2 and concomitant unrestricted passage of CH_4, CO, and N_2 through the pores of the framework. Such experiments using binary gas mixtures such as CO_2/CH_4, CO_2/CO, and CO_2/N_2 (50:50 v/v) were carried out in a column packed with activated ZIF-68−70, -78−82, -95, or -100 at room temperature. The resultant breakthrough curves reveal that only CO_2 is retained while the other gas passes through without hindrance. For example, calculations indicate that ZIFs have higher selectivity for CO_2 in CO_2/CO gas mixtures than the industrially pertinent BPL carbon, thus supporting the potential applicability of using these ZIFs as selective CO_2 reservoirs.[13−16]

Recent studies showed that hydrogen is attracted to the imidazole backbone of the ZIF structure.[25] In light of these findings, the active pursuit of ZIFs constructed from the diverse array of imidazole building units will undoubtedly produce materials with novel gas adsorption properties. Because it is now commonly believed that anthropogenic carbon dioxide emissions need to be abated, research into the potential utility of ZIFs as practical CO_2 capture materials has intensified.

Perspective and Outlook

The impact of link−link interactions on the choice of topology coupled with the extensive library of known functionalized imidazolate links has led to a large class of diverse ZIF materials. Given that there are millions of possible tetrahedral structures and that ZIF synthesis is amenable to high-throughput methods, there remains a very rich chemistry to be explored. Additionally, the trend in ZIF chemistry from materials discovery to the design of complex structures is clearly evident in the development of ZIFs comprised of mixed links with different chemical functionalities and through the exploration of isoreticular covalent functionalization of the organic framework. The chemical stability of ZIFs and the vast number of organic reactions that potentially can be effected on the crystals suggest that, as in the case of molecular chemistry, links may be chemically modified to perform specific functions. For example, the introduction of ligand-binding moieties into the pore space of ZIFs via isoreticular covalent functionalization will facilitate binding of metal ions that will act to enhance gas adsorption and separation properties and to potentially perform size- and shape-selective catalysis. Continued research into transferring the concepts of molecular reaction chemistry to the solid state in order to synthesize ZIFs with complex pore functionalities will indubitably lead to structures with tailored functionality. The flexibility with which ZIF structures can be made and functionalized, coupled to their stability, bodes well for designing ZIFs capable of not only capturing carbon dioxide but also transforming it into a fuel.

We acknowledge the innovative contributions of the following from the Yaghi research group: Drs. Kyosung Park, Ni Zheng, Bo Wang, Rahul Banerjee, Adrien Côté, Hideki Hayashi, Hiroyasu Furukawa, Prof. Hee Chae (Seoul National University), and Mr. Will Morris. This work was partially supported by DOE-BES, and as part of the Center for Gas Separations Relevant to Clean Energy Technologies, an Energy Frontier Research Center funded by the U.S. Department of Energy, Office of Science, Office of Basic Energy Sciences under Award Number DE-SC0001015.

Supporting Information Available. Larger high-resolution images of crystal structures of ZIFs. This material is available free of charge via the Internet at http://pubs.acs.org.

BIOGRAPHICAL INFORMATION

Anh Phan was born in 1971 in Hue, Vietnam. She received her B.S. in chemistry in 2005 from the University of California—Berkeley where she performed research with Prof. Kenneth Raymond. She is currently pursuing a Ph.D. degree at the University of California—Los Angeles under the direction of Prof. Omar Yaghi. Her research mainly focuses on the discovery of new porous materials that have been constructed from tetrahedral transition metals and imidazolate and their applications in gas storage and catalysis.

Christian J. Doonan was born in Geelong, Australia, in 1976. He received his Ph.D. from the University of Melbourne with Prof. Charles G. Young. He is currently a postdoctoral fellow with Prof. Omar Yaghi at UCLA. His research involves using reticular chemistry principles to develop new open framework materials.

Fernando J. Uribe-Romo was born in 1983 in Ensenada, Baja California, México. He obtained his B.S. in Chemistry in 2006 from the Instituto Tecnológico y de Estudios Superiores de Monterrey (ITESM), Campus Monterrey, Nuevo León, México. He is currently a Ph.D. student at the University of California—Los Angeles with Prof. Omar Yaghi. His current research includes the crystallization of new porous materials constructed exclusively of strong bonds.

Carolyn B. Knobler was born in 1934 in New Brunswick, New Jersey. She received her B.S. in chemistry (1955) from the George Washington University and Ph.D. (1958) from the Pennsylvania State University. She is currently a Research Chemist at UCLA. Her specialty is crystallography.

Michael O'Keeffe was born in 1934 in Bury St Edmunds, England. He received a B.Sc. in chemistry (1954), Ph.D. (1958), and D.Sc. (1976) degrees from the University of Bristol where he studied with Professor F. Stone. In 1963, he joined Arizona State University where he is now Regents' Professor of Chemistry. He is currently with the Center for Reticular Chemistry at the California NanoSystems Institute. His recent research is devoted particularly to the theory of three-periodic structures relevant to development of taxonomy of such structures and its application to materials design and description.

Omar M. Yaghi was born in Amman, Jordan, in 1965. He received his Ph.D. from the University of Illinois—Urbana (1990) with Professor Walter G. Klemperer. He was an NSF Postdoctoral Fellow at Harvard University with Professor Richard H. Holm (1990−1992). He is currently Irving and Jean Stone Professor in Physical Sciences, Professor of Chemistry and Biochemistry, and Professor of Molecular and Medical Pharmacology at UCLA, where he directs the Center for Reticular Chemistry. He has established several research programs dealing with the reticular synthesis of discrete polyhedra and extended frameworks from organic and inorganic building blocks.

FOOTNOTES

*To whom correspondence should be addressed. E-mail: yaghi@chem.ucla.edu.

REFERENCES

1 Maesen, T. L. M.; Marcus, B. In *Introduction to Zeolite Science and Practice*; van Bekkum, H., Flanigen, E. M., Jacobs, P. A., Jansen, J. C., Eds.; Elsevier: Amsterdam, 2001; pp 1−9.

2 The term link−link interactions is inclusive of all the potential influences that may occur between the organic links in solution such as, hydrogen bonding, $\pi-\pi$ attractions, and steric interference.

3 Liu, Y.; Kravtsov, V. Ch.; Larsen, R.; Eddaoudi, M. Molecular Building Blocks Approach to the Assembly of Zeolite-Like Metal-Organic Frameworks (ZMOFs) with Extra-Large Cavities. *Chem. Commun.* **2006**, 1488–1490.

4 Huang, X.-C.; Lin, Y.-Y.; Zhang, J.-P.; Chen, X.-M. Ligand-Directed Strategy for Zeolite-Type Metal-Organic Frameworks: Zinc(II) Imidazolates with Unusual Zeolitic Topologies. *Angew. Chem., Int. Ed.* **2006**, *45*, 1557–1559.

5 Zhang, J.-P.; Chen, X.-M. Crystal engineering of binary metal imidazolate and triazolate frameworks. *Chem. Commun.* **2006**, 1689–1699.

6 Rettig, S. J.; Storr, A.; Summers, D. A.; Thompson, R. C.; Trotter, J. Iron(II) 2-Methylimidazolate and Copper(II) 1,2,4- Triazolate Complexes: Systems Exhibiting Long-Range Ferromagnetic Ordering at Low Temperatures. *Can. J. Chem.* **1999**, *77*, 425–433.

7 Tian, Y.-Q.; Cai, C.-X.; Ji, Y.; You, X.-Z.; Peng, S.-M.; Lee, G.-H. $[Co_5(im)_{10} \cdot 2MB]_\infty$: A Metal-Organic Open-Framework with Zeolite-Like Topology. *Angew. Chem., Int. Ed.* **2002**, *41*, 1384–1386.

8 Tian, Y.-Q.; Cai, C.-X.; Ren, X.-M.; Duan, C.-Y.; Xu, Y.; Gao, S.; You, X.-Z. The Silica-Like Extended Polymorphism of Cobalt(II) Imidazolate Three-Dimensional Frameworks: X-ray Single-Crystal Structures and Magnetic Properties. *Chem.—Eur. J.* **2003**, *9*, 5673–5685.

9 Masciocchi, N.; Bruni, S.; Cariati, E.; Cariati, F.; Galli, S.; Sironi, A. Extended Polymorphism in Copper(II) Imidazolate Polymers: A Spectroscopic and XRPD Structural Study. *Inorg. Chem.* **2001**, *40*, 5897–5905.

10 Huang, X.; Zhang, J.; Chen, X. $[Zn(bim)_2] \cdot (H_2O)_{1.67}$: A Metal-Organic Open-Framework with Sodalite Topology. *Chin. Sci. Bull.* **2003**, *48*, 1531–1534.

11 Park, K. S.; Ni, Z.; Côté, A. P.; Choi, J. Y.; Huang, R.; Uribe-Romo, F. J.; Chae, H. K.; O'Keeffe, M.; Yaghi, O. M. Exceptional Chemical and Thermal Stability of Zeolitic Imidazolate Frameworks. *Proc. Natl. Acad. Sci. U.S.A.* **2006**, *103*, 10186–10191.

12 Zhang, J.; Wu, T.; Zhou, C.; Chen, S.; Feng, P.; Bu, X. Zeolitic Boron Imidazolate Frameworks. *Angew. Chem., Int. Ed.* **2009**, *48*, 2542–2545.

13 Hayashi, H.; Côté, A. P.; Furukawa, H.; O'Keeffe, M.; Yaghi, O. M. Zeolite a Imidazolate Frameworks. *Nat. Mater.* **2007**, *6*, 501–506.

14 Banerjee, R.; Phan, A.; Wang, B.; Knobler, C.; Furukawa, H.; O'Keeffe, M.; Yaghi, O. M. High-Throughput Synthesis of Zeolitic Imidazolate Frameworks and Application to CO_2 Capture. *Science* **2008**, *319*, 939–943.

15 Wang, B.; Côté, A. P.; Furukawa, H.; O'Keeffe, M.; Yaghi, O. M. Colossal Cages in Zeolitic Imidazolate Frameworks as Selective Carbon Dioxide Reservoirs. *Nature* **2008**, *453*, 207–212.

16 Banerjee, R.; Furukawa, H.; Britt, D.; Knobler, C.; O'Keeffe, M.; Yaghi, O. M. Control of Pore Size and Functionality in Isoreticular Zeolitic Imidazolate Frameworks and Their Carbon Dioxide Selective Capture Properties. *J. Am. Chem. Soc.* **2009**, *131*, 3875–3877.

17 Baerlocher, Ch.; Meier, W. M.; Olson, D. H. *Atlas of Zeolite Framework Types*, 6th revised ed.; Elsevier: Amsterdam, 2007.

18 Baburin, I. A.; Leoni, S.; Seifert, G. Enumeration of Not-Yet-Synthesized Zeolitic Zinc Imidazolate MOF Networks: A Topological and DFT Approach. *J. Phys. Chem. B* **2008**, *112*, 9437–9443.

19 Wang, Z.; Cohen, S. M. Postsynthetic Modification of Metal-Organic Frameworks. *Chem. Soc. Rev.* **2009**, *38*, 1315–1329.

20 Ingleson, M. J.; Arrio, J. P.; Guilbaud, J.-B.; Khimyak, Y. Z.; Rosseinsky, M. J. Framework Functionalisation Triggers Metal Complex Binding. *Chem. Commun.* **2008**, 2680–2682.

21 Morris, W.; Doonan, C. J.; Furukawa, H.; Banerjee, R.; Yaghi, O. M. Crystals as Molecules: Postsynthesis Covalent Functionalization of Zeolitic Imidazolate Frameworks. *J. Am. Chem. Soc.* **2008**, *130*, 12626–12627.

22 Sircar, S. Basic Research Needs for Design of Adsorptive Gas Separation Processes. *Ind. Eng. Chem. Res.* **2006**, *45*, 5435–5448.

23 Llewellyn, P. L.; Bourrelly, S.; Serre, C.; Vimont, A.; Daturi, M.; Hamon, L.; Weireld, G. D.; Chang, J.-S.; Hong, D.-Y.; Hwang, Y. K.; Jhung, S. H.; Férey, G. High Uptakes of CO_2 and CH_4 in Mesoporous Metal—Organic Frameworks MIL-100 and MIL-101. *Langmuir* **2008**, *24*, 7245–7250.

24 Millward, A. R.; Yaghi, O. M. Metal—Organic Frameworks with Exceptionally High Capacity for Storage of Carbon Dioxide at Room Temperature. *J. Am. Chem. Soc.* **2005**, *127*, 17998–17999.

25 Wu, H.; Zhou, W.; Yildirim, T. Hydrogen Storage in a Prototypical Zeolitic Imidazolate Framework-8. *J. Am. Chem. Soc.* **2007**, *129*, 5314–5315.

26 Tian, Y.-Q.; Zhao, Y.-M.; Chen, Z.-X.; Zhang, G.-N.; Weng, L.-H.; Zhao, D.-Y. Design and Generation of Extended Zeolitic Metal-Organic Frameworks (ZMOFs): Synthesis and Crystal Structures of Zinc(II) Imidazolate Polymers with Zeolitic Topologies. *Chem.—Eur. J.* **2007**, *13*, 4146–4154.

27 Lehnert, V. R.; Seel, F. Preparation and Crystal Structure of the Manganese(II) and Zinc(II) Derivative of Imidazole. *Z. Anorg. Allg. Chem.* **1980**, *464*, 187–194.

28 Sturm, M.; Brandl, F.; Engel, D.; Hoppe, W. Crystal Structure of Diimidazolylcobalt. *Acta Crystallogr.* **1975**, *B31*, 2369–2378.

29 Masciocchi, N.; Ardizzoia, G. A.; Brenna, S.; Castelli, F.; Galli, S.; Maspero, A.; Sironi, A. Synthesis and Ab-Initio XRPD Structure of Group 12 Imidazolato Polymers. *Chem. Commun.* **2003**, 2018–2019.

30 Tian, Y.-Q.; Xu, L.; Cai, C.-X.; Wei, J.-C.; Li, Y.-Z.; You, X.-Z. Determination of the Solvothermal Synthesis Mechanism of Metal Imidazolates by X-ray Single-Crystal Studies of a Photoluminescent Cadmium(II) Imidazolate and Its Intermediate Involving Piperrazine. *Eur. J. Inorg. Chem.* **2004**, 1039–1044.

31 Tian, Y.-Q.; Chen, Z.-X.; Weng, L.-H.; Guo, H.-B.; Gao, S.; Zhao, D. Y. Two Polymorphs of Cobalt(II) Imidazolate Polymers Synthesized Solvothermally by Using One Organic Template *N,N*-Dimethylacetamide. *Inorg. Chem.* **2004**, *43*, 4631–4635.

32 Huang, X.-C.; Zhang, J.-P.; Lin, Y.-Y.; Yu, X.-L.; Chen, X.-M. Two Mixed-Valence Copper (I, II) Imidazolate Coordination Polymers: Metal-Valence Tuning Approach for New Topological Structures. *Chem. Commun.* **2004**, 1100–1101.

33 Rettig, S. J.; Storr, A.; Summers, D. A.; Thompson, R. C.; Trotter, J. Transition Metal Azolates From Metallocenes. Synthesis, X-ray Structure, and Magnetic Properties of a Three-Dimensional Polymetallic Iron(II) Imidazolate Complex, a Low-Temperature Weak Ferromagnet. *J. Am. Chem. Soc.* **1997**, *119*, 8675–8680.

34 Rettig, S. J.; Sanchez, V.; Storr, A.; Thomson, R. C.; Trotter, J. Polybis(4-Azabenzimidazolato)-Iron(II) and Cobalt(II). 3-D Single Diamond-Like Framework Materials Which Exhibit Spin Canting and Ferromagnetic Ordering at Low Temperatures. *J. Chem. Soc., Dalton Trans.* **2000**, 3931–3937.

35 Liu, Y.; Kravtsov, V. Ch.; Eddaoudi, M. Template-Directed Assembly of Zeolite-Like Metal-Organic Frameworks (ZMOFs): A usf-ZMOF with an Unprecedented Zeolite Topology. *Angew. Chem., Int. Ed.* **2008**, *47*, 8446–8449.

36 Wu, T.; Bu, X.; Zhang, J.; Feng, P. New Zeolitic Imidazolate Frameworks: From Unprecedented Assembly of Cubic Clusters to Ordered Cooperative Organization of Complementary Ligands. *Chem. Mater.* **2008**, *20*, 7377–7382.

37 Muller-Buschbaum, K. A Three-Dimensional Network With Complete Nitrogen Coordination Obtained From an Imidazole Melt. *Z. Naturforsch. B: Chem. Sci.* **2006**, *61*, 792–798.

38 Fu, Y.-M.; Zhao, Y.-H.; Lan, Y.-Q.; Wang, Y.; Qiu, Y.-Q.; Shao, K.-Z.; Su, Z.-M. A Chiral 3D Polymer With Right- and Left-Helices Based on 2,2′-Biimidazole: Synthesis, Crystal Structure and Fluorescent Property. *Inorg. Chem. Commun.* **2007**, *10*, 720–723.

39 Lorente, M. A. M.; Dahan, F.; Petrouleas, V.; Bousseksou, A.; Tuchagues, J.-P. New Ferrous Complexes Based on the 2,2′-Biimidazole Ligand: Structural, Moessbauer, and Magnetic Properties of $[Fe^{II}(bimH_2)_2(CH_3OH)_2](OAc)_2$, $[Fe^{II}(bimH_2)_3]CO_3$, $[Fe^{II}(bimH_2)_2]_n$, and $\{[Fe^{II}(bim)]\}_n$. *Inorg. Chem.* **1995**, *34*, 5346–5357.

40 Han, J.-Y.; Fang, J.; Chang, H.-Y.; Dong, Y.; Liang, S. Poly[μ_2-4,4′-Bipyridine-di-μ_2-Imidazolido-Cadmium(II)]. *Acta Crystallogr.* **2005**, *E61*, m2667—m2669.

41 Lehnert, V. R.; Steel, F. Crystal Structure of the Iron(II) Derivative of Imidazole. *Z. Anorg. Allg. Chem.* **1978**, *444*, 91–96.

42 Spek, A. L.; Duisenberg, A. J. M. The Structure of the Three-Dimensional Polymer Poly[μ-Hexakis(2-Methylimidazolato-N, N')-Triiron(II)], $[Fe_3(C_4H_5N_2)_6]_n$. *Acta Crystallogr.* **1983**, *C39*, 1212–1214.

43 Wu, T.; Bu, X.; Liu, R.; Lin, Z.; Zhang, J.; Feng, P. A New Zeolitic Topology with Sixteen-Membered Ring and Multidimensional Large Pore Channels. *Chem.—Eur. J.* **2008**, *14*, 7771–7773.

44 Method of analysis: The Cambridge Structural Database was searched with the criterion of obtaining all the structures that contain the metal—bi-imidazole; the metal is surrounded by at least four nitrogens, two of which are part of the imidazole ring. Each imidazole is bound to two metals through the nitrogen atoms with no discrimination according to the nature of the bonds. Recently published compounds were obtained from the CCDC deposition number. This search gave a total of 172 structures, which were analyzed with the *TOPOS* 4.0 package [Blatov, V. A.; Carlucci, L.; Ciani, G.; Proserpio, D. M. Interpenetrating Metal-Organic and Inorganic 3D Net Works: A Computer-Aided Systematic Investigation. Part I Analysis of the Cambridge Structural Database. *CrystEngComm* **2004**, *6*, 377—395]. For each entry, all doubled atoms were eliminated, and the adjacency matrix was calculated using the AutoCN routine with the default parameters and excluding hydrogen bonds, van der Waals, and special contacts. The obtained database was filtered to eliminate all the zero-, one-, and two-dimensional structures; 105 structures were found to be three-dimensional. The adjacency matrix was then simplified by calculating the centroids with the *ADS* routine for all non-metal atoms, and then all 0-, 1- and 2-connected atoms were eliminated, obtaining a database that includes only the reduced graphs of the nets. The topology of the reduced structures was obtained using the *ADS* routine with the default parameters, selecting the "classification" option for only valence bonds. In some cases, the topology was obtained using *Systre 1.1.5* [Delgado-Friedrichs, O.; O'Keeffe, M. Identification of, and Symmetry Computation for Crystal Nets. *Acta Crystallogr.* **2003**, *A59*, 351—360].

45 O'Keeffe, M.; Peskov, M. A.; Ramsen, S. J.; Yaghi, O. M. The Reticular Chemistry Structure Resource (RCSR) Database of, and Symbols for, Crystal Nets. *Acc. Chem. Res.* **2008**, *41*, 1782–1789.